

Electrochemical impedance spectroscopy characterization of Cobalt oxide decorated silicon nanowires

Madjid IFIRES^{#*1}, Toufik HADJERSI^{#2}, Redouane CHEGROUNE^{#3}, Sabrina LAMRANI^{#4}, Brahim IDIR^{**5}, Amar MANSERI^{#6}

[#]Research Center in Semi-conductor Technology for the Energetic, CRTSE - 02, Bd. Dr. Frantz FANON, B.P. 140 Alger-7 Merveilles 16038, Algeria

¹ifires.madjid@crtse.dz

²hadjersitoufik@crtse.dz

⁴Lamrani.S@crtse.dz

⁶mansriamar@crtse.dz

^{*}Département de Sciences des Matériaux, Faculté de Génie Mécanique et Génie des Procédés, USTHB, B.P. 32 El-Alia, 16111, Bab-Ezzouar, Algeria

³chegroune_redouane@yahoo.fr

^{**} Centre de Recherche en Technologies Industrielles, (CRTI) BP 64, Route de Dely Brahim, Chéraga 16014 Alger - Algeria

⁵b.idir@csc.dz

Abstract— The silicon nanowires (SiNWs) modified with cobalt oxide were prepared by electrodeposition. Surface characteristics and electrochemical properties of anodically electrodeposited cobalt on SiNWs were investigated by scanning electron microscope and electrochemical impedance spectroscopy. The impedance spectroscopic responses of cobalt coated silicon nanowires were characterized by three time relaxation processes related to three distinct capacitance peaks. When the potential was increased for oxygen evolution reaction (OER), the R_{ct} values of the cobalt oxide coated SiNWs decreases gradually from 10 to $k\Omega$. The cobalt oxide nanosheets could serve as a site for oxygen evolution electrocatalysts with improved property compared to unmodified SiNWs.

Keywords—Silicon, nanowires, cobalt oxide, electrocatalysts.

I. INTRODUCTION

Silicon is an attractive material for splitting reaction by oxidation or reduction of water which imply the oxygen and the hydrogen evolution, respectively [1]. Recently, silicon nanowires have received a great deal attention in reason of their volume/surface ratio that allows to have a high specific surface which leads to the high water splitting reaction efficiency. Indeed, it is reported that water oxidation on SiNWs photoanode, on which a thin layer of TiO_2 was deposited by atomic layer deposition (ALD), exhibits a high photocurrent (2.5 times greater than planar Si/ TiO_2) [2]. Also, significant photoelectrochemical reactivity on Ir/ TiO_2 / Si nanocomposites was observed [3]. In addition, it is shown

that the silicon/hematite core/shell nanowire array decorated with Au nanoparticles offers a great promise for water oxidation without external bias voltage [4]. Huang et al. reported the spin coated of reduced graphene oxide (rGO) on top of SiNWs exhibits an enhanced properties of hydrogen evolution reaction (HER) compared to that of planar rGO/Si composite [5]. The enhanced properties of HER of the SiNWs@ MoS_3 composite [6] and SiNWs@Co [7, 8] also were reported in the literature.

It is well known that precious metals oxides such as IrO_2 , RuO_2 and Nb_2O_5 are the best electrocatalysts in neutral or weakly acidic solutions for oxygen evolution reaction (OER) [9-13]. Unfortunately, these materials are very expensive.

However, Cobalt oxides in particular the nanocrystalline spinel are highly active electrocatalysts and chemical stable in alkaline electrolytes [14-20]. These two properties made that these materials are commode for oxygen evolution reaction (OER), given that the Co oxide dissolves in acidic media [21]. Consequently, it is very important to realize an electrocatalyst anode based on SiNWs and CoO_x in order to combine their interesting properties to provide a best performance as anode electrode.

In this paper, we study the electrochemical behavior of n-SiNWs modified by cobalt oxide in neutral or slightly basic media by impedance spectroscopy.

II. EXPERIMENTAL

Silicon nanowires (SiNWs) were fabricated via two-step metal-catalyzed electroless etching (MACE) [22-24]. First, the n-Si (100) wafers were degreased by sonication in acetone and ethanol, rinsed with deionized water, and then cleaned in a piranha solution (3:1 concentrated $\text{H}_2\text{SO}_4/30\% \text{H}_2\text{O}_2$) for 10 min, followed by copious rinsing with deionized water. The thin oxide layer formed on the surface was then etched in a 10% HF solution for 5 min. After, these samples were dipped for 1 min into an aqueous solution composed of 4.8 M HF and 0.05 M AgNO_3 to electroless deposit of Ag nanoparticles (AgNPs). Subsequently, these coated samples were immersed for 1 h, in etching solution composed of 4.8 M HF and 0.4 H_2O_2 . After the etching, the SiNWs samples were covered with Ag dendrites and nanoparticles, which were removed by immersion into aqueous HNO_3 solution (65%) during 5 min. Finally, the samples were rinsed with deionized water and dried under a gentle stream of nitrogen.

The obtained SiNWs serve as a substrate on which we deposit the cobalt oxide by anodic deposition in the electrolyte of 0.001 M $\text{CoCl}_2 \cdot (\text{H}_2\text{O})_6$, 0.001 M KCl and 0.01 M H_3BO_3 . The deposition was carried out at room temperature, in a three electrode cell. A platinum foil was used as counter electrode and an Ag/AgCl electrode as reference. The anodic electrodeposition was performed by varying the potential from 0.5 to 1.6 V vs. Ag/AgCl. All EIS and linear sweep voltammetry (LSV) experiments were carried out by using an aqueous 0.1 M Na_2SO_4 solution at 25 °C.

The EIS measurements were performed using an Autolab potentiostat/galvanostat in the frequency range 100 mHz–100 kHz. The measurement potential range was between open circuit potential (OCP) and 1.60 V (Ag/AgCl). A 10 mV amplitude of sinusoidal potential perturbation was employed.

SEM images and EDX spectra of the films were obtained using a Philips SEM 505 microscope.

III. RESULTS AND DISCUSSION

A. MORPHOLOGY

The most conducted experiments for water oxidation catalysis were in acidic and alkaline solutions. However, substrate and nanowires of Si degrade rapidly in alkaline solutions, for that reason the experiments were conducted in neutral sulfate solution.

The morphology of MACE fabricated SiNWs were illustrated in Fig. 1. From Fig. 1a, it is seen that the Si is uniformly covered with nanowires after etching for 1 h. Also, it can be observed that the nanowires tips stick together, forming bundles. The initial bending could be due to surface tensional forces which are effective during the drying process. Subsequently, the van der Waals forces hold the nanowires together [22, 23]. The length of nanowires is about 30 μm measured from cross-sectional view SEM image (not shown

here). From the Fig. 1b, one can observe that the length of SiNWs decreases to about 9 μm after EIS and linear sweep voltammetry (LSV) experiments in 0.1 M Na_2SO_4 . This means that the nanowires were etched from their tips.

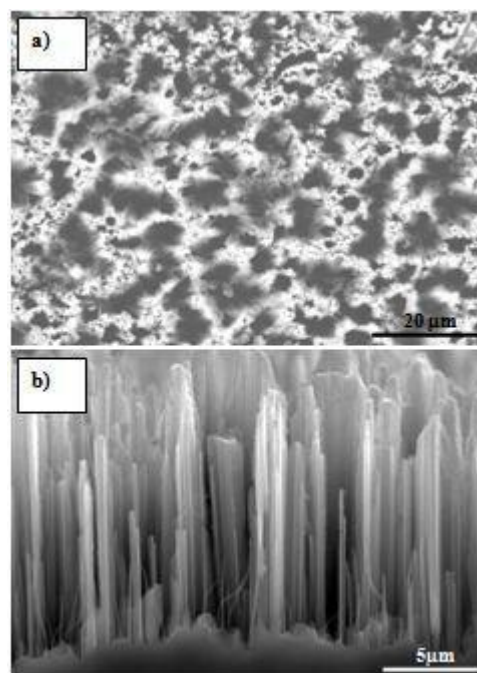


Fig. 1 Plan (a) and cross-sectional (b) view SEM images of SiNWs: (a) just as synthesized and (b) after LSV and electrochemical impedance measurement in 0.1 M Na_2SO_4 .

The morphology of CoO_x electrodeposited on SiNWs was characterized by SEM, as shown in Figs. 2a and b. They show that the CoO_x deposit on SiNWs layer in the shape of nanosheets. This shape prevents the deeper penetration which is limited at about 5 μm . It can be noted that the SiNWs length decreases of a manner not significant compared to the previous case. This means that the Co oxide acts as protector against the dissolution of SiNWs tips.

The chemical composition of the CoO_x modified SiNWs were examined using energy dispersive X-ray analysis (Fig. 2c). The results show that the analysed layer was composed of only Si, O, and Co, suggesting that the CoO_x was deposited onto SiNWs.

B. ELECTROCHEMICAL CHARACTERIZATION

The electrochemical impedance spectra were illustrated in Fig. 3. The Nyquist diagrams and Bode plots of SiNWs at various applied anodic potentials in 0.1 M Na_2SO_4 were shown in Fig. 3 (a and b).

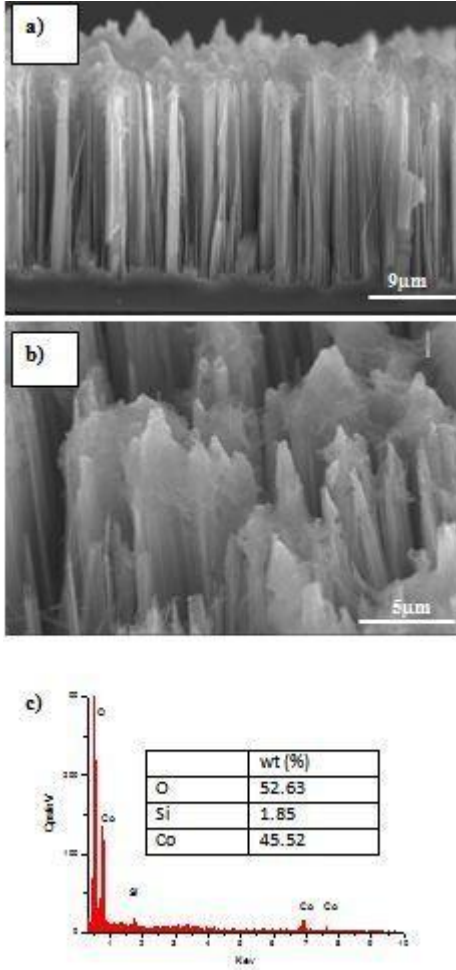


Fig. 2 : Cross-sectional view SEM images at low (a) and high (b) magnification of n-SiNWs modified with CoOx. (c) is an energy-dispersive X-ray spectrum of CoO_x deposited onto silicon nanowires.

The first pseudo semi-circle appeared at high frequencies $\sim 10^5$ Hz as it can be seen in the inset of the Fig. 3a. This can be attributed to the junction Si/SiO₂. The same behavior was observed by Sari et al. [25]. The second semi-circle appeared at frequencies about 10^3 Hz regions which is related to the bulk resistance. The last one appears at low frequencies ~ 10 Hz which can be ascribed to the charge transfer and strongly depends on the applied bias voltage.

The results of the fitted electrochemical impedance spectra were showed in TABLE I. The R1 represents the bulk resistance combined with capacitance C1 of the interface SiO₂/Si which corresponds to first pseudo semi-circle in

Nyquist plots and first peak in Bode plots. The same results were reported by Sari et al. [25]. The combined R2 in parallel with the capacitance C2 represent the interface SiO₂/CoO_x which correspond to second semi-circle in Nyquist plots and the second peak in Bode plots as illustrated in Figs. 3 and 4.

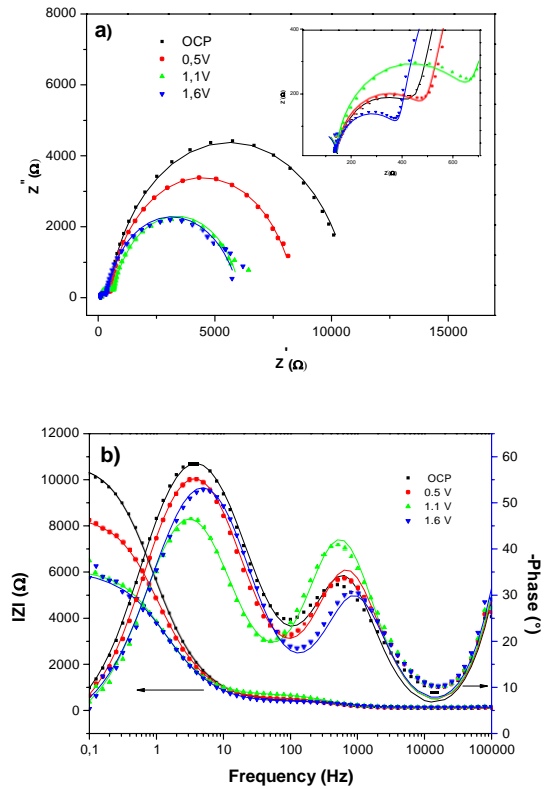


Fig. 3 Electrochemical impedance spectra of SiNWs at different applied potential, a) Nyquist plot, b) bode plot in 0.1 M Na₂SO₄. The scatters show the experimental data, and lines show the results of fitting to the equivalent circuit in Fig. 5. The inset in figure 1a is an enlarged of the origin.

The last elements R3 and C3 represent the charge transfer resistance and the capacitance of CoO_x modified SiNWs, respectively. The latter depend on the voltage bias over 0.5 V as illustrated in the table 1. It is very difficult to explain this behavior which needs more detailed studies. The CPE element is used to describe the non-homogeneity of the electrode surface. The impedance of the CPE is defined as:

$$Z_{CPE}=[Y_0(j\omega)^n]^{-1}$$

Where Y_0 is the CPE constant phase element, n is the CPE power and ω is the angular frequency. The Fig.5 shows the equivalent circuit.

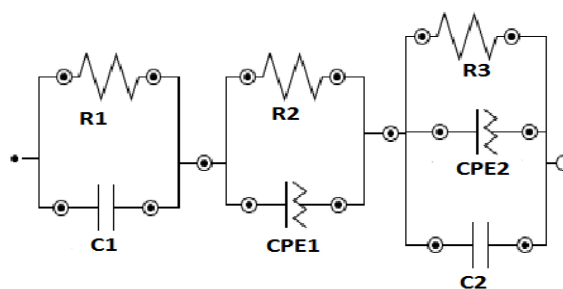


Fig. 4 Equivalent circuit used to simulate the electrochemical impedance spectra of SiNWs and CoO_x modified SiNWs.

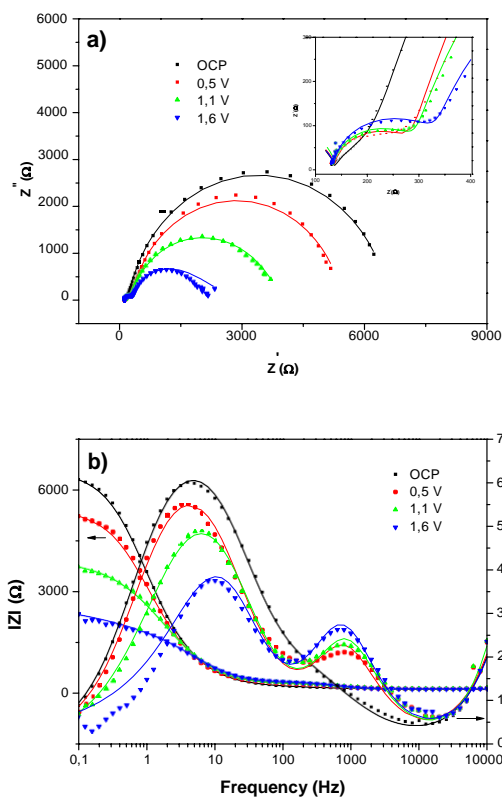


Fig. 4 Electrochemical impedance spectra of CoO_x modified SiNWs at different applied potential, a) Nyquist plots, b) bode plots in 0.1 M Na_2SO_4 . The scatters show the experimental data, and lines show the results of fitting to the equivalent circuit in Fig. 5.

The TABLE I indicates that the charge transfer resistance decreases by increasing of the bias voltage and it is related to the oxygen evolution reaction. The values of this resistance drastically decrease when SiNWs are modified with CoO_x . This decrease can be related to the oxidation of the Co^{2+} and Co^{3+} toward Co^{4+} as reported recently in the literature [26, 27].

To better understand the OER process on silicon substrate and CoO_x modified SiNWs, we performed LSV measurements. The figure 6 shows LSV spectra CoO_x modified SiNWs for different voltage scanning rate. The apparent pic which its intensity increases with voltage scanning rate is probably attributed to a combination of the formation of a passivating film of $\text{Co}(\text{OH})_2$ and /or CoO as reported by Lyons et al. [28].

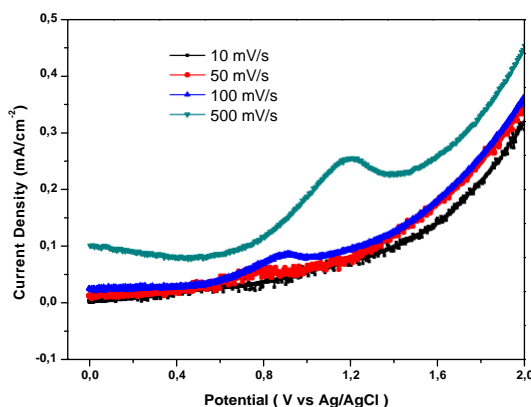


Fig. 5 Linear sweep voltammetry of CoO_x modified SiNWs at different scanning rate.

IV. CONCLUSIONS

A combination of scanning electron microscopy, linear sweep voltammetry, Electrochemical impedance was used to investigate the oxygen evolution reaction (OER) occurring on the surface of cobalt oxide deposited on SiNWs.

It is found that the electrodeposited CoO_x film can provide best performances and can act as anode with high catalytic performance. In addition, it protects the SiNWs tips from the dissolution and increases the conductivity of SiNWs.

The authors gratefully acknowledge the financial support from General Direction of Scientific Research and of Technological Development of Algeria (DGRSDT/MESRS).

ACKNOWLEDGMENT

TABLE. 1 Summary of fitted EIS data of CoO_x decorated SiNWs at various applied potentials

Element	nSiNWs				SiNWs/CoO _x				
	Potential (V vsAg/AgCl)	OCP	0,5	1,1	1,6	OCP	0,5	1.1	1.6
R1 (Ω)		144	143	142	140	79,3	139	134	135
CPE1(μMho)		0.00147	1.51	1.56	1.66	50,4	2,04	1.21	4,11
n1		1	1	1	1	0,753	-	1	-
C2 (μF)		1,5	1,23	1,21	1,17	0.00429	0.00431	1,76	1,69
R2		297	338	512	244	134	136	154	196
C3 (μ F)		0.009	0.009	3,79	15	0.009	0.009	15,6	20,2
R3 (K Ω)		10,374	7,96	5,45	5,73	6,39	5,19	3,69	2,53
CPE3 (μMho)		27,869	31,4	36,4	26,5	43,2	48,8	47,3	141
n3		0,892	0,898	0,878	0,72	0,885	0,874	0,669	0,351

REFERENCES

- [1] S.Y. Reece, J. A. Hamel, K. Sung, T.D. Jarvi, A. J.Esswein, J.J.H. Pijpers, D.G. Nocera, Wireless Solar Water Splitting Using Silicon-Based Semiconductors and Earth-Abundant Catalysts, *Science.*, vol. 334, pp. 645–648, 2011.
- [2] Y. J. Hwang, A. Boukai, and P. Yang, High Density n-Si/n-TiO₂ Core/Shell Nanowire Arrays with Enhanced Photoactivity, *Nano Lett.*, vol. 9, pp. 410–415, 2009.
- [3] Y. Chen, J. D. Prange, S. Dühren, Y. Park, M. Gunji, C. E. D. Chidsey and P. C. McIntyre, Atomic layer-deposited tunnel oxide stabilizes silicon photoanodes for water oxidation, *Nat. Mater.*, vol. 10, pp. 539–544, 2011.
- [4] X. Wang, K-Q. Peng, Y. Hu, F-Q. Zhang, B. Hu, L. Li, M. Wang, X-M. Meng, and S.-T. Lee, Silicon/Hematite Core/Shell Nanowire Array Decorated with Gold Nanoparticles for Unbiased Solar Water Oxidation, *Nano Lett.*, vol. 14, pp. 18–23, 2014.
- [5] Z. Huang, P. Zhong, C. Wang, X. Zhang, and C. Zhang, Silicon Nanowires/Reduced Graphene Oxide Composites for Enhanced Photoelectrochemical Properties, *ACS Appl. Mater. Interfaces.*, vol. 5, pp. 1961–1966, 2013.
- [6] Z. Huang, C. Wang, L. Pan, F. Tian, X. Zhang, C. Zhang, Enhanced photoelectrochemical hydrogen production using silicon nanowires@MoS₃, *Nano Energy.*, vol. 2, pp. 1337–1346, 2013.
- [7] L. Zhao, K. Liao, M. Pynenburg, L. Wong, N. Heinig, J. P. Thomas, and K.T. Leung, -Electro-oxidation of Ascorbic Acid by Cobalt Core-Shell Nanoparticles on a H-Terminated Si(100) and by Nanostructured Cobalt-Coated Si Nanowire Electrodes, *ACS Appl. Mater. Interfaces.*, vol. 5, pp. 2410–2416, 2013.
- [8] X. Bao, M. F. Cerqueira, P. Alpuim and L. Liu, -Silicon Nanowire Arrays Coupled with Cobalt Phosphide Spheres as a Low-Cost Photocathode for Efficient Solar Hydrogen Evolution, *Chem. Commun.*, vol. 51, pp. 10742–10745, 2015.
- [9] M. Yagi, E. Tomita, S. Sakita, T. Kuwabara, K. Nagai, -Self-Assembly of Active IrO₂ Colloid Catalyst on an ITO Electrode for Efficient Electrochemical Water Oxidation, *J. Phys. Chem. B.*, vol. 109, pp. 21489–2149, 2005.
- [10] E. Tsuji, A. Imanishia, K.-I. Fukuia Y. Nakato, -Electrocatalytic activity of amorphous RuO₂ electrode for oxygen evolution in an aqueous solution, *Electrochim. Acta.*, vol. 56, pp. 2009–2016, 2011.
- [11] J.-M. Hu, J.-Q. Zhang C.-N. Cao, -Oxygen evolution reaction on IrO₂-based DSA® type electrodes: kinetics analysis of Tafel lines and EIS, *Int. J. Hydrogen Energy.*, vol. 29, pp. 791–797. 2004.
- [12] Z. Mou, S. Yin, M. Zhu, Y. Du, X. Wang, P. Yang, J. Zheng and C. Lu, -RuO₂/TiSi₂/graphene composite for enhanced photocatalytic hydrogen generation under visible light irradiation, *Phys.Chem. Chem. Phys.*, vo. 15, pp. 2793–2799, 2013.
- [13] M.H.P. Santana, L.A. De Faria, -Oxygen and chlorine evolution on RuO₂+TiO₂+ CeO₂+Nb₂O₅ mixed oxide electrodes, *Electrochim. Acta.*, vol. 51, pp. 3578-3585, (2006).
- [14] F. Cheng, J. Shen, B. Peng, Y. Pan, Z. Tao, J. Chen, -Rapid room-temperature synthesis of nanocrystalline spinels as oxygen reduction and evolution electrocatalysts, *Nat. Chem.*, vol. 3, pp. 79–84, 2011.

- [15] F. Jiao , H. Frei, -Nanostructured Cobalt Oxide Clusters in Mesoporous Silica as Efficient Oxygen-Evolving Catalysts, *Angew. Chem. Int. Ed.*, vol. 48, pp. 1841–1844, 2009.
- [16] T. W. Kim, M. A. Woo, M. Regis, and K.-S. Choi, -Electrochemical Synthesis of Spinel Type ZnCo₂O₄ Electrodes for Use as Oxygen Evolution Reaction Catalysts, *J. Phys. Chem. Lett.*, vol. 5, pp. 2370–2374, 2014.
- [17] X. Z. Shu , M. Zhang , Y. He , H. Frei , F. D. Toste , -Dual Visible Light Photoredox and Gold-Catalyzed Arylative Ring Expansion, *J. Am. Chem. Soc.*, vol. 136, pp. 5844–5847, 2014.
- [18] M. Zhang, M. de-Respini , H. Frei, -Time-resolved observations of water oxidation intermediates on a cobalt oxide nanoparticle catalyst, *Nat. Chem.*, vol. 6, pp. 362–367, 2014.
- [19] H. S. Soo , A. Agiral , A. Bachmeier , H. Frei, -Visible Light-Induced Hole Injection into Rectifying Molecular Wires Anchored on Co₃O₄ and SiO₂ Nanoparticles, *J. Am. Chem. Soc.*, vol. 134, pp. 17104–17116, 2012.
- [20] N. Sivasankar , W. W. Weare , H. Frei, -Direct Observation of a Hydroperoxide Surface Intermediate upon Visible Light-Driven Water Oxidation at an Ir Oxide Nanocluster Catalyst by Rapid-Scan FT-IR Spectroscopy, *J. Am. Chem. Soc.*, vol. 133, pp. 12976–12979, 2011.
- [21] J. Chivot, L. Mendoza, C. Mansour, T. Pauporte, M. Cassir, New insight in the behaviour of Co-H₂O system at 25-150°C, based on revised Pourbaix diagrams, *Corros. Sci.*, vol. 50, pp. 62-69, 2008.
- [22] S. Lamrani, A. Guittoum, R. Schäfer, M. Hemmou, V. Neud, S. Pofahl, T. Hadjersi, N. Benbrahim, -Morphology, structure and magnetic study of permalloy films electroplated on silicon nanowires, *J. Magn. and Magn. Mater.*, vol. 396, pp. 263–267, 2015.
- [23] O. Fellahi, M. R. Das, Y. Coffinier, S. Szunerits, T. Hadjersi, M. Maamache and R. Boukherroub, -Silicon nanowire arrays-induced graphene oxide reduction under UV Irradiation, *Nanoscale*, vol. 3, pp. 4662–4669, 2011.
- [24] S. K. Srivastava, D. Kumar, P.K. Singh, M. Kar, V. Kumar, M. Husain, -Excellent antireflection properties of vertical silicon nanowires arrays, *Solar Energy Materials & Solar Cells*, vol. 94, pp. 1506–1511, 2010.
- [25] H. Sari, H. Sakakura, D. Kawade, M. Itagaki, M. Sugiyama, -Quantification of sputtering damage during NiO film deposition on a Si/SiO₂ substrate using electrochemical impedance spectroscopy, *Thin Solid Films*, vol. 592, pp. 150–154, 2015.
- [26] B.S. Yeo and A. T. Bell, -Enhanced Activity of Gold-Supported Cobalt Oxide for the Electrochemical Evolution of Oxygen, *J. Am. Chem. Soc.* Vol. 133, pp. 5587–5593, 2011.
- [27] S. A. Bonke, M. Wiechen, R. K. Hocking, X.-Y. Fang, D.W. Lupton, D. R. Mac Farlane, and L. Spiccia, -Electrosynthesis of Highly Transparent Cobalt Oxide Water Oxidation Catalyst Films from Cobalt Aminopolycarboxylate Complexes, *Chem. Sus. Chem*, vol. 24, pp. 1394–1403, 2015.
- [28] M. E. G. Lyons, M. P. Brandon, -The Oxygen Evolution Reaction on Passive Oxide Covered Transition Metal Electrodes in Alkaline Solution Part II – Cobalt, *Int. J. Electrochem. Sci.*, Vol. 3, pp. 1425 – 1462, 2008.